Lab on a Chip

Accepted Manuscript

This is an *Accepted Manuscript*, which has been through the Royal Society of Chemistry peer review process and has been accepted for publication.

Accepted Manuscripts are published online shortly after acceptance, before technical editing, formatting and proof reading. Using this free service, authors can make their results available to the community, in citable form, before we publish the edited article. We will replace this *Accepted Manuscript* with the edited and formatted *Advance Article* as soon as it is available.

You can find more information about *Accepted Manuscripts* in the **Information for Authors**.

Please note that technical editing may introduce minor changes to the text and/or graphics, which may alter content. The journal's standard **Terms & Conditions** and the **Ethical guidelines** still apply. In no event shall the Royal Society of Chemistry be held responsible for any errors or omissions in this *Accepted Manuscript* or any consequences arising from the use of any information it contains.

ARTICLE TYPE

A flow-free droplet-based device for high throughput polymorphic crystallization

Shih-Mo Yang[a,b], Dapeng Zhang[a], Wang Chen[a], and Shih-Chi Chen[a]*

[a] Department of Mechanical and Automation Engineering and Shun Hing Institute of Advanced Engineering, The Chinese University of
5 Hong Kong, Hong Kong

[b] Complex and Intelligent Research Center, School of Mechanical and Power Engineering, East China University of Science and
Technology, Shanghai, PR China

*Corresponding author: scchen@mae.cuhk.edu.hk

Crystallization is one of the most crucial steps in the process of pharmaceutical formulation. In recent years, emulsion-based platforms have been developed and broadly adopted for generating high quality products. However, these conventional approaches such as stirring
15 are still limited in several aspects, e.g., unstable crystallization conditions and broad size distribution; besides, only simple crystal forms can be produced. In this paper, we present a new flow-free droplet-based formation process for producing highly controlled crystallization with two examples: (1) NaCl crystallization reveals the ability of packaging saturated solution into nano-liter droplets, and (2) glycine crystallization demonstrates the ability of producing polymorphic crystallization forms by controlling the droplet size and temperature. In our process, the saturated solution automatically fills the microwell array powered by degassed bulk PDMS. A critical oil
20 covering step is then introduced to isolate the saturated solution and control the water dissolution rate. Utilizing surface tension, the solution is uniformly packaged in the form of thousands of isolating droplets at the bottom of each microwell of 50 - 300 µm diameter. After water dissolution, individual crystal structures are automatically formed inside the microwell array. This approach facilitates the study of different glycine growth processes: α- form generated inside the droplets and γ- form generated at the edge of the droplets. With precise temperature control over nano-liter-sized droplets, the growth of ellipsoidal crystalline agglomerates of glycine was achieved for
25 the first time. Optical and SEM images illustrate that the ellipsoidal agglomerates consist of 2 - 5µm glycine clusters with inner spiral structures of ~35µm screw pitch. Lastly, the size distribution of spherical crystalline agglomerates (SAs) produced from microwells of different sizes was measured to have a coefficient variation (CV) of less than 5%, showing crystal sizes can be precisely controlled by microwell sizes with a high uniformity. This new method can be used to reliably fabricate monodispersed crystals for pharmaceutical applications.

30

Introduction

Crystallization is one of the most crucial steps in the process of pharmaceutical formulation as it determines not only the growth
35 and size distribution of polymorphic forms, but also affects the drug bioperformance.[1] Furthermore, the crystallization characters, e.g., crystal form and structure size/shape, attribute to the drug effects of the active pharmaceutical ingredient (API); accordingly, a well-controlled crystallization process is highly needed.
40 Currently, several issues remain unresolved such as energy consumption, the unpredictability of crystal forms, and the lack of uniformity in crystal growth.[2] To address these challenges, Kawashima group proposed the use of emulsion-based API crystallization to directly form spherical agglomeration with
45 controlled sizes. They have achieved the formation of salicylic acid crystals within dispersed droplets in an immiscible continuous phase.[3]

Polymorphic glycine is usually investigated to understand API for
50 the following reasons: (1) its three crystal forms, α–, β–, and

γ– are widely known, (2) its crystal growth can be well controlled by adjusting the pH value of the solution, and (3) amino-acid is often applied as a model molecule for the API study.[4-6] Currently a number of methods for crystallization process are in use. For
55 example, the emulsion-based method which involves stirring aqueous glycine-in-oil is useful for the crystallization of polymorphic forms and the attachment of silicon nanoparticles to surface of glycine-based spherical crystalline agglomerates (SAs).[7,8] Alternatively, the microfluidic-based approach, which
60 involves generating individual droplets from a concentric microfluidic glass capillary, is relatively well-controlled to achieve size uniformity of SAs.[9]

While these methods have their respective advantages such as
65 high throughput or uniform crystal size, there are some limitations when it comes to the performance of polymorphic crystallization. For example, stirring the mixture of a glycine/water solution generates a broad size distribution as the crystals tend to gather together as they grow, despite of the
70 benefit of a large number of microemulsions for α–, β–, and γ– forms of glycine crystals. Moreover, the crystal growth rate and

crystal size are not easily controlled since the crystallization process occurs continuously in the environment of a bulk saturated solution.[7,10]

The use of microfluidic-based platform, a highly monodispersed fluid surrounded by another immiscible fluid, provides the possibility of forming a large quantity of uniform, small volume droplets by adjusting the flow rate of dispersed and continuous phases.[11] While the throughput of droplet production is enormous, i.e., a yield rate reaching kHz range from femtoliter to nanoliter scale,[12] the system setup, typically including a syringe pump, connecting tubes and flow switches/microvalves, is complex to build and control. Especially when the quantity of droplets is great, such design can be inconvenient to arrange or pattern droplets in arrays for product screening even with the help of bypass microchannel network and specific geometric structure.[13-15] Moreover, it is inevitable that when the droplets are driven in a microchannel, the local vortices can induce unwanted shear force inside the droplets, which results in an unstable aqueous environment that can affect the quality of crystal products. To be more specific, spherical crystallization occurs easily after the shrinkage of a moving droplet containing saturated glycine solution; nevertheless, single α– and γ– glycine crystals do not grow easily in unstable circumstances.[8,9] For static parallel operation, Lee et al. proposed to confine droplet arrays based on functionalized gold islands with hydrophilic surfaces[16]; however, in this device supersaturated droplets are directly exposed to air, resulting in high evaporation rate and rough crystal quality. To improve pharmaceutical crystallization, therefore, it is imperative to develop new high throughput processes that will satisfy the needs for rapid isolation of reagent to be formed as droplets. In addition, the process should ensure a stable environment for high quality crystal growth and produce highly uniform products with effective temperature control.

In this article, we present an efficient flow-free method to generate high quality products in crystallization processes. The method involves the following steps: (1) an aqueous saturated solution is filled automatically into the cavities; (2) the liquid is isolated and formed automatically as droplets; (3) instead of using a liquid driving mechanism, our design creates a static condition inside droplets. The results demonstrate uniformity of products, high throughput, clear and complete structure of single crystals, and the crystallization of ellipsoidal glycine structure for the first time.

Materials and methods

Device fabrication

The mold for crystallization chip was fabricated with standard lithographic processes. A microwell array was defined by using a negative photoresist (SU-8). After exposure and development, a 100 µm tall mold was fabricated on a silicon substrate. The elastomer base and the curing agent of PDMS (Sylgard 184, Dow Corning, USA) were mixed together in the proportion of 10:1. After degassing, the mixture was poured onto the SU-8 mold and cured at 70°C for 120 minutes. Finally, the cured PDMS structure was separated from the mold and the microwell array was fabricated on the chip. The array contains 1,330 round cavities of 100 µm diameter over a 1 x 1 cm^2 area.

Materials and temperature conditions

In order to generate pure single crystals, NaCl and glycine were dissolved in deionized water respectively at room temperature (25 ℃) to the saturation point without adding other reagents. In the glycine crystallization experiments, two temperature conditions were used to control crystal growth in microwells:

Temperature process 1 (TP1): a saturated solution was placed on the surface of degassed PDMS at room temperature (25℃). After the solution filled the cavities of microwells for 5 minutes, the solution was drawn out and then covered with mineral oil immediately. The chip was kept at steady room temperature for water dissolution to take effect.

Temperature process 2 (TP2): a saturated solution was prepared and kept at 90℃. A degassed microchip was placed on a hot plate for 5 minutes in order to bring its temperature to that of the saturated solution. Next, the saturated solution was placed on the PDMS surface for the liquid to fill the microwells. After 5 minutes, the solution was drawn out and then covered with mineral oil immediately. The bulk PDMS was kept on the hot plate for another 10 to 15 minutes before it was removed to cool down to the room temperature.

Droplet package procedure

PDMS has the character of air permeability and contains very little air in its bulk volume.[17,18] When the air within is removed, the bulk PDMS can absorb air from its surroundings. Owing to such feature, the bulk PDMS chip was degassed in advance in vacuum conditions for 30 minutes. When the chip surface was covered with liquid, the gas in the microwells would start to permeate slowly into the PDMS bulk, thus reducing the air pressure in the cavities. As the degassed PDMS absorbed the air, the actual air volume reduced accordingly. As the gas pressure started to differ, the liquid was driven into the microwell automatically, as shown in Fig. 1(a) and (b). Note that the PDMS's ability to absorb air is subject to the time it requires to be degassed during the vacuum treatment. The longer it takes to degas the bulk PDMS, the faster it increases the gas absorption velocity; our experience indicates that 50 minutes of vacuum treatment is sufficient.

Next, the liquid on the chip surface was removed, the solution inside microwells was contained by the surface tension, and mineral oil was applied to cover the whole chip surface, as shown in Fig. 1(c). This oil covering step made the trapped solution to separate from air and embedded in mineral oil surrounding. Once the mineral oil covered the microwells, the conditions of the three phases changed from air/aqueous/solid to oil/aqueous/solid. Finally, the difference in the net surface tension reached a new

balance, and the embedded aqueous solution shrank to a form a spheroid inside the microwell, shown in Fig. 1(d).

In theory, when the water molecules inside the droplets dissolve in a mineral oil environment at room temperature, the volume of droplets reduces slowly. Based on the aforementioned theory, the water dissolution and the subsequent volume reduction brought the concentration of the droplet to supersaturation and led to nucleation/crystallization eventually, as shown in Fig. 1(e). [19,20] Finally, as water dissolved completely in the oil environment, a clear and transparent crystal was formed and placed in an individual microwell, as shown in Fig. 2(f). In this method, both of the slow water dissolution and stable droplet shrinkage process contributed to the crystal quality. It is worth noting that in the previously reported SlipChip method the supersaturated solution is prepared and confined in solid surrounding, i.e. glass cavities.[14] Since glass cannot absorb water molecules in the supersaturated solution, the solute concentration decreases over the crystallization process, resulting in early termination of crystal growth.
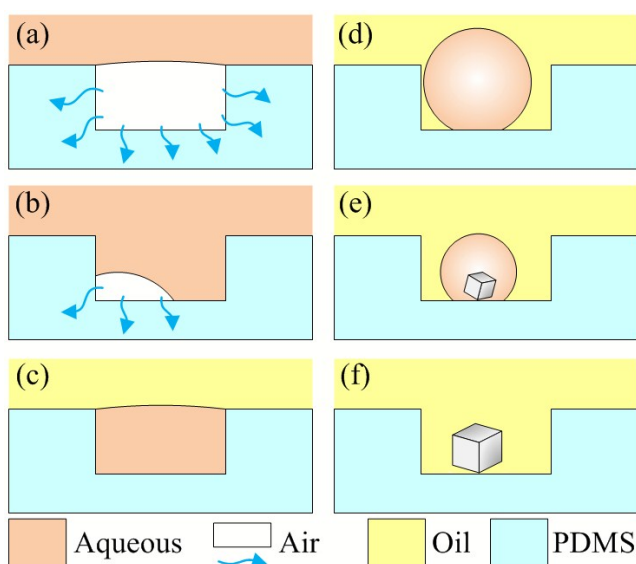
Figure 1. (a)(b) When the aqueous phase covered the chip surface, the degassed PDMS absorbed the trapped air. (c) After the aqueous solution was removed, the oil covered the chip surface and a small volume of liquid was isolated and packaged inside the microwell cavity. (d) Droplet formation: surface tension force caused the trapped liquid to form a spheroid shape at the bottom of the cavity. (e) Water extraction: the water molecules dissolved slowly into the oil surrounding. When the volume of saturated droplet reduced, crystallization occurred and the crystal was formed in the cavity. (f) The water molecules entirely dissolved in the oil environment, and a clear and transparent crystal was formed at the bottom of each microwell due to the slow water dissolution.

Droplet volume and contact angle

In this section, we measured the diameter of droplets and calculated their volume so as to identify the amount of the contained aqueous solution. Figure 2(a) illustrates a droplet adhered to a planar surface. By assuming the spheroidal droplets take the form of a perfect sphere, the actual droplet volume can be estimated by Equation (1) below:

$$V = \frac{\pi}{3}\left[2R^3 + (2R^2 + r^2)\sqrt{R^2 - r^2}\right] \quad (1)$$

where R = the radius of the sphere and r = the radius of the round contact area between the droplet and the substrate. The relationship between R and r can be determined by measuring their respective lengths shown on top-view microscopic images. The volume ratio of a droplet adhering to a substrate and a free droplet can be obtained by dividing Eq. (1) by $V_{sphere}=(4\pi R^3)/3$. Due to the different properties of saturated NaCl and glycine solution, their respective relationships with surface tensions balance lead to different r/R ratios. Based on the microscopic images, the r/R ratios of NaCl and glycine are 0.25 and 0.8 respectively. By substituting these ratios into previous relationship, we can find the respective droplet volumes of NaCl and glycine are 99.93% and 89.6% of a complete sphere. As such, we are able to precisely estimate the actual volume of a droplet by measuring its radius as well as the radius of its contact area.

Contact angle is an important parameter of surface tension for quantifying the wettability when a liquid/vapor interface meets a solid substrate. Traditionally, the contact angle is measured by analyzing the side-view photos of droplets placed on a planar surface. In our work, we analyzed the top-view photos instead because the aqueous droplets were embedded and adhered in cylindrical cavities. Figure 2(b) shows the schematic diagram of the balanced surface tension forces among aqueous, oil and solid phases. According to the geometric relationship between R and r as shown in Fig. 2(a), one can derive the equation for contact angle θ_c as

$$r = R|sin\theta_c| \quad (2)$$

Based on the aforementioned r/R ratios, the respective contact angles of saturated NaCl droplet and glycine droplet embedded in mineral oil are about 165° and 127°.
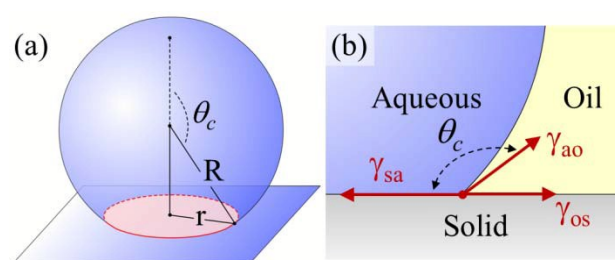
Figure 2. Schematic diagram of a trapped droplet. (a) R and r represent the respective radii of the droplet and the round aqueous/solid interface. (b) Balance of contact angle and surface tension forces among aqueous, oil and solid phases. Contact angle can be obtained by measuring the length of R and r.

Lab on a Chip
CREATED USING THE RSC ARTICLE TEMPLATE (VER. 3.0) - SEE WWW.RSC.ORG/ELECTRONICFILES FOR DETAILS
Page 4 of 8

ARTICLE TYPE
www.rsc.org/xxxxxx | XXXXXXXX

Experimental Results and Discussion

In this section, we present the packaging and crystallization process of (1) NaCl and (2) glycine. For NaCl, all processes were performed at TP1 (25℃), where the dissolution/crystallization
5 process typically takes a few days to complete. For the saturated glycine solution, two temperature conditions were set, 25℃ and 90℃, to generate various crystal structures, e.g., plane, needle, cone, spherical crystalline agglomerates (SAs), and ellipsoidal crystalline agglomerates (EAs). These new processes have
10 substantially improved the capability for indexing individual droplets and enabled the investigation of individual polymorphic forms.

Packaging NaCl solution into droplets

15 The process of high throughput droplet formation is shown in Fig. 3(a) - (f) First, a saturated NaCl solution covered the degassed PDMS and some air was inevitably trapped in the microwells, Fig. 3(a). As the degassed PDMS gradually absorbed the gas, the volume of the trapped air reduced, thus forming a concave
20 air/liquid surface, Fig. 3(b). Figure 3(c) shows the last gas bubble at the bottom of microwell after 5 minutes of gas absorption. Once the liquid fully filled the cavities, the NaCl solution was removed and the mineral oil was subsequently dropped onto the chip surface, Fig. 3(d). Due to surface tension, the trapped NaCl
25 solution in the mineral oil shrank and gradually formed spheroidal droplets, as in Fig. 3(e). Finally, inside each microwell a droplet was formed within 30 seconds, and the surface tension between the oil and aqueous interface forced the droplet to adhere to the bottom of the microwell, as in Fig. 3(f).

30
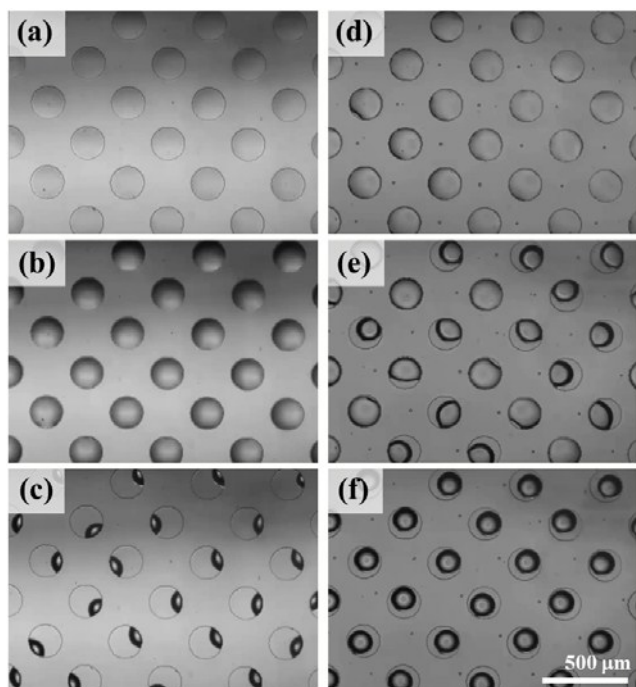
Figure 3. The procedure of aqueous droplet formation. (a) First,
the NaCl solution covered the surface of the microwell array.
t=0s. (b) The trapped air was absorbed into the degassed PDMS-
35 based structure, creating a concave aqueous/air interface. t=45s.

(c) A remaining small air bubble was absorbed at the bottom of the microwells. t=210s. A total of 330 seconds was required for the bulk PDMS to absorb all air bubbles in the 200 μm-diameter microwells (d) Mineral oil covered the PDMS surface to package
40 NaCl solution inside the microwells. (e)(f) Surface tension caused the embedded NaCl solution to shrink and form droplets. A single droplet was generated in each microwell. It took about 30 seconds to form the droplet array from the moment when PDMS was covered with oil. This process was captured in the video and
45 provided in the supporting information.

NaCl crystallization

Figure 4(a) - (c) show the formation and growth of NaCl crystals within the droplets contained in individual microwells. In the
50 beginning, the volume of each droplet was similar. After the two-day incubation, the droplet volume reduced and a single crystal nucleated within the droplets. Figure 4(a) illustrates the NaCl crystals with each of them resided in a microwell. Despite of the different growth rates among crystals, the slow water dissolution
55 process ensures clear and transparent crystals can be formed with good uniformity. Figure 4(b) shows that a cubic crystal was formed in a droplet adhering to the substrate of the microwell after three days of incubation. Figure 4(c) shows a single crystal formed in the microwell after four days of incubation, where in
60 the picture the incident light was reflected through its flat surfaces as four light bars in the microwell.
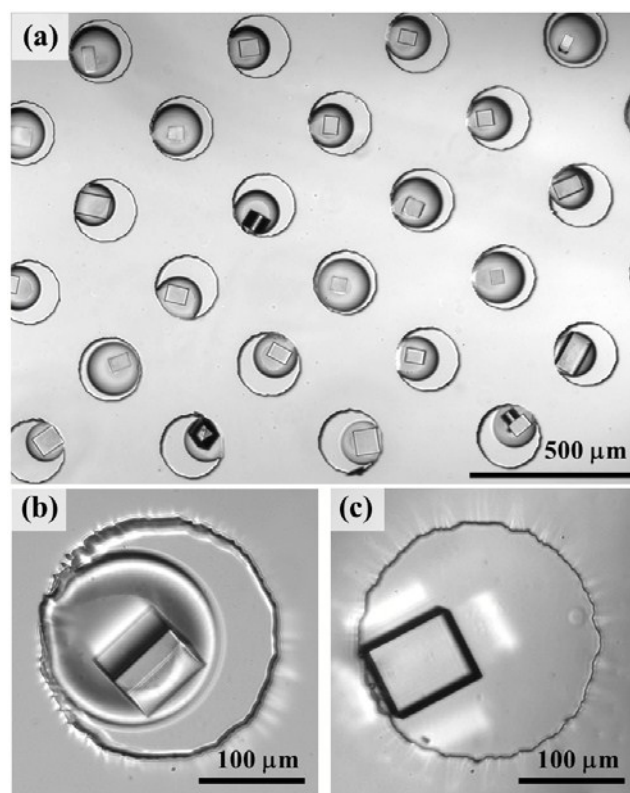
65 Figure 4. Arrays of NaCl crystal nucleation and crystal growth. (a) After the water molecules gradually dissolved into the oil, NaCl crystals formed inside the droplets after two days of incubation. (b) A zoom-in view of a single crystal formed in a droplet inside

microwell. (c) A single cubic NaCl crystal formed after six days of incubation with a clear cubic structure.

Figure 5 presents a bar chart showing the tendency of higher
5 dissolution rate for smaller droplets due to its higher surface area to volume ratio. To quantify the water dissolution rate, we calculated the volume of droplets within microwells of 100μm, 200μm, and 300μm diameters respectively at different time points, namely day 0, day 2 and day 4. The ratio of average
10 droplet volume reduction is estimated as following

$$R_V = \frac{V_{initial} - V_{final}}{V_{initial} \times Time} \times 100\%$$

where '*Time*' = 2 days. $V_{initial}$ and V_{final} = the droplet volume at different time points. In the beginning, or at Day 0, the average droplet volume inside the 100μm, 200μm, and 300μm diameter
15 microwells were 0.30 nano-liter, 2.72 nano-liter, and 6.68 nano-liter respectively. The respective droplet reduction ratios are about 18%, 14%, and 9%. This result confirms that higher surface area to volume ratio will result in higher dissolution rate.
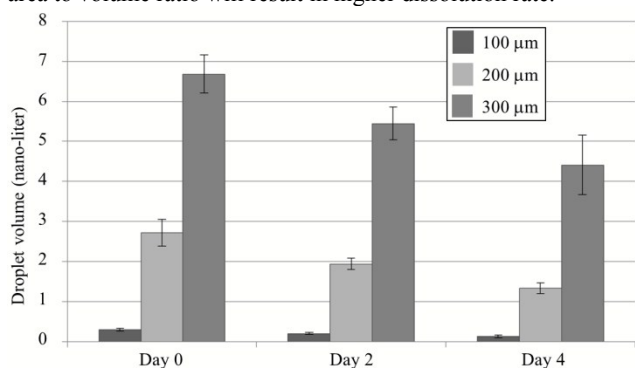
20 Figure 5. Droplet volume reduction in microwells of 100μm, 200μm, and 300μm diameters. While bigger droplets dissolve more water, smaller droplets still experience faster water dissolution rate.

Glycine crystallization
In this section, we present the experimental results of glycine crystallization, where glycine was first dissolved in deionized water to a saturated state without additives or reagents. Then, glycine crystals were formed using the droplet platform and
30 observed with optical microscopes. The results show α-, γ-glycine SAs were formed randomly under TP1 condition and EAs were crystallized under TP2 condition.

α–form glycine
35 Figure 6(a) - (d) illustrate a set of typical α–form crystals growing in droplets and (e) - (h) show the completed crystals inside 200μm diameter microwells. The rule to identify crystal forms is based on the well-known α–glycine structure: plate, bipyradim, lamella, or needle-like shapes.[5-7,21] The α– crystal
40 growth period is approximately 1 - 2 days. In addition, the crystallization process can be influenced, or accelerated, by existing glycine crystals. In other words, when a crystal nucleates inside a droplet, the droplet volume reduces faster than those

without crystals. These results were found with our new droplet-
45 based platform, which enables indexing products in designated locations so as to facilitate observations and analyses.
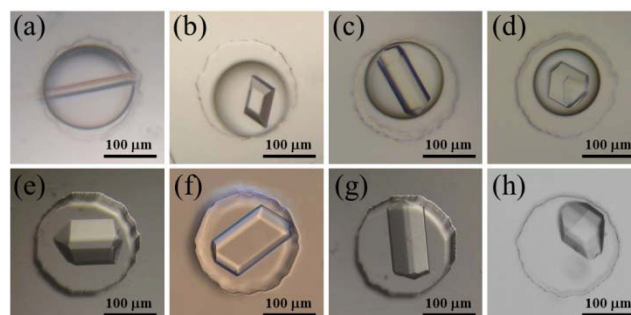
Figure 6. α–form glycine crystals. (a) - (d) Growth of glycine
50 crystals inside droplets. The slow water dissolution process provides stable conditions for the growth of single and complete glycine crystal. (e) - (h) After ~1 day of growth, a single glycine crystal was formed in the microwell. Its morphology exhibited the features of α–form glycine, e.g., plate, bipyradim, lamella, or
55 needle-like shapes.

γ–form glycine
The growth of single γ-form glycine with our droplet-based method marks a significant difference from the use of bulk
60 solution or stirring processes. One distinguishing character of γ–crystals is its polar morphology. Due to the positive and negative molecule charges of the glycine structure, γ–form crystals grow faster along the direction of COO^- (–c), and slower along directions where NH_3^+ (+c) is rich.[5,22] Such difference in crystal
65 growth rate makes the γ–form structure specific, which is flat at one end and pointed at the other end. Our experiments show that the γ–form growth at the point end stopped, while the flat end $[COO^- (–c)]$ continuously crystallized at the interface between itself and the attaching droplet, as shown in Fig. 7(a). Comparing
70 to α–form crystallization, this is a very different phenomenon because α–form always occurs inside the droplet. Therefore, the triangular pyramid structure is a character very specific to the γ–form of glycine crystal for identification puropose.[7,21,23]

75 Figure 7(b) shows a single γ–form glycine observed from its pointed end. Our crystallization method can generate two cone structures attached together, with their two points aligning towards the same direction, as shown in Fig. 7(c) and (d). It means a re-growth phenomenon of γ–form crystal: while the cone
80 crystal remains inside the saturated glycine droplet, a new nucleation point can occur on the flat surface of the original cone structure. As the water continues to dissolve, the second cone structure grows whereas the original cone crystal stops to grow. Moreover, multi-cone structures of γ–form glycine may occur
85 occasionally. Figure 7(f) - (h) demonstrate two, three and four cone structures growing towards different directions with their points contacting with one another. Although these types of γ–form glycine crystal formation may seem difficult to be identified, the unique cone structure still makes them distinguishable.

90
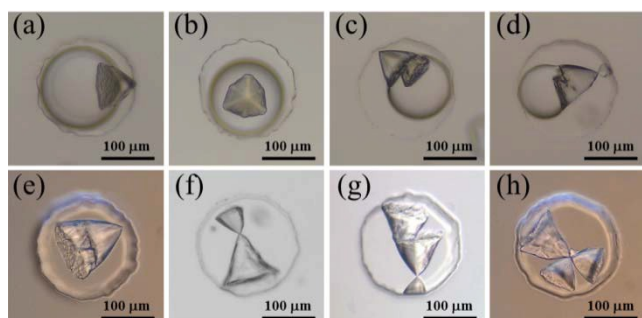
Figure 7. γ–form glycine crystals. (a) - (d) The growth of the γ–form crystal attached to the surface of a glycine-saturated droplet inside a 200μm diameter microwell. (e) A single γ– form glycine

5 crystal. (f) - (h) Various types of γ–glycine crystals. The unique characteristic of γ– form is manifested: slower and shorter growth forming a pointed end along the NH_3^+ direction as well as faster and longer growth forming a flat end along the COO^- direction. The flat end [COO^- (−c)] of γ–glycine crystals always attaches to

10 the droplet.

Spherulitic and ellipsoidal agglomerates

In this experiment, we set different temperatures, TP1 and TP2, as control conditions to produce SAs and EAs (Fig. 8). First, the

15 temperature is a crucial operative condition because it affects droplet volume shrinkage and water dissolution of glycine solution emulsions. According to previous publications, the SAs crystallization occurs when the emulsions are placed on an 84℃ hot plate.[7,9] Nonetheless, our results demonstrate that the SAs of

20 glycine can be generated at room temperature (25℃) as well. As evidenced in Fig. 9(b), all α– , γ–, and SAs are formed on the same chip. Second, SAs nucleate faster in comparison with the crystal growth rate of α– and γ– glycine. In the case of α– and γ– glycine crystals, the droplet volume diminishes within 1 - 2 days

25 and the crystals are attached to the droplets. Nevertheless, once the glycine concentration reaches supersaturation, SAs start to nucleate, growing so rapidly that they fully fill the droplet and form a spherical structure. Our method allows easy observation of different glycine growth rates.

30

Formation of SAs and EAs under TP1 condition

The microwell array not only promotes the crystallization throughput but also provides a convenient and effective method for indexing products over a relatively large area, as the NaCl and

35 glycine crystals demonstrated in Fig. 9. Thousands of NaCl crystals were formed on a single chip with each of them located in individual microwells after three days, Fig. 9(a). Figure 9(c) shows the results of SAs under TP1 condition inside the 100μm diameter microwell array. The small droplet volume is

40 accountable for such throughput because it is easier for a small volume droplet, ~300 pico-liter, to reach the supersaturation state.

Glycine crystallization under TP1 condition in the 200μm diameter microwell array was also investigated, as shown in Fig.

45 9(b). Note that while most of the crystal forms are γ–, the formation of α–, γ– and SA on the same chip is still achievable and their growths do not influence each other as droplets are packaged in individual microwells. In other words, regardless of

current publications' finding that spherical glycine structure is to

50 be generated at high temperature, e.g., ~80℃. Our results prove that SAs generation is attainable at room temperature.
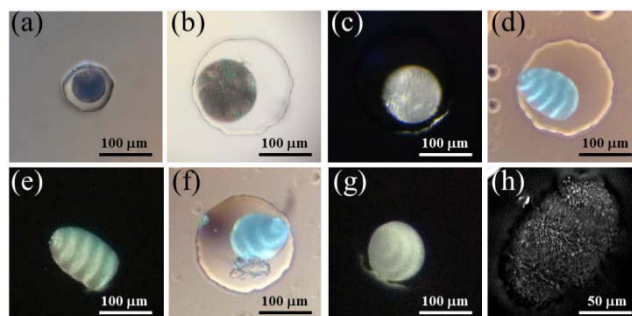
Figure 8. Brightfield and darkfield microscopic images of SAs

55 and EAs. (a) - (c) Single SAs located inside100μm and 200μm diameter microwells. (d), (e) Images and the reflected light pattern of spiral crystalline obtained under the condition of rapid temperature drop. (f), (g) The reflection pattern at the end of EAs revealing the tip of the inner spiral structure. (h) EAs composed

60 of tiny needle-like glycine crystals with widths of 2 - 5μm.

Formation of EAs under TP2 condition

Through experiments and observation, we found ellipsoidal glycine structures can be produced with a rapid temperature drop.

65 This condition can be met with our droplet-based platform using TP2 condition. Under TP2, the droplet at 90℃ had a higher saturated concentration than that at room temperature. When the device was removed from the hot plate, the fast temperature drop induced the growth of EAs. We learn with surprise that under

70 TP2 condition, the shape of agglomerate structure is ellipsoidal with inner spiral crystalline, as shown in Fig. 8(d) - (g). The microscopic images reveal that the respective lengths of SAs' major axis and minor axis are ~150μm and ~90μm. The reflected light from the inner crystal cluster then illuminated the spiral

75 structure clearly with a screw pitch of ~35 μm at both ends of the EAs structure, shown in Fig. 8(f) and 8(g). A desktop SEM (Phenom G2) was used to examine the size and surface morphology of the EAs. Figure 8(h) shows that the EA structure was composed of numerous long and tiny needle-like glycine

80 crystals with widths of about 2 - 5μm. Based on the darkfield and brightfield images of EAs' surface, layers of crystal cluster grew in different directions, as shown in Fig. 8(d) - (g).

This is the first report to employ two temperature conditions, TP1

85 and TP2, to induce SAs and EAs formation. By means of our flow-free droplet-based platform, the growth of agglomerates of glycine crystal consisting of α– and β– forms can all be achieved.[7,9,24] The investigation on the inner components of SAs and EAs as well as their crystallization mechanism is ongoing.

90
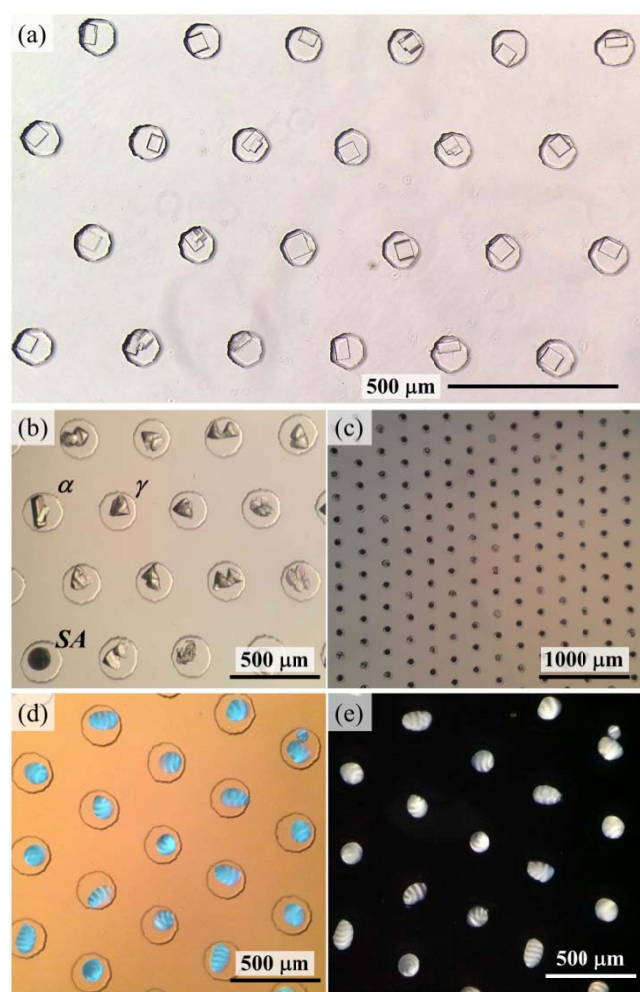
Figure 9. Images of NaCl and glycine crystals produced by the droplet-based platform. (a) Single cubic NaCl crystals were generated in individual microwells. (b) A single SA formed on the same chip of α− and γ− glycine crystals indicating that SAs can be generated at room temperature. (c) Arrays of SAs crystallization products in the 100μm diameter microwells. (d) & (e) Brightfield and darkfield images of EAs array product, showing good uniformity in crystallization process.

In the last experiment, we like to demonstrate that precise and uniform SAs production can be achieved by selecting appropriate microwell dimensions. This is important as uniformity is essential when a large number of crystals are generated in pharmaceutical production. Figure 10 illustrates the size distribution of the SAs inside the 50μm, 100μm, 200μm, and 300μm diameter microwells. Theoretically, the size of SAs is subject to the amount of aqueous solution confined inside the droplet whose volume shrinks from the column volume of a microwell cavity. We measured the diameter of two hundred SAs; and the mean particle size of the SAs in the 50μm, 100μm, 200μm, and 300μm diameter microwells is 41μm, 72μm, 122μm, and 181μm respectively with a standard deviation of 1.6μm, 3.2μm, 5.4μm, and 9.7μm. The coefficient of variance (CV) is low, CV < 5%, indicating that the size of SAs can be controlled by defining the volume of microwells. In other words, using microwells to control product size has been proved to be reliable in the crystallization process.
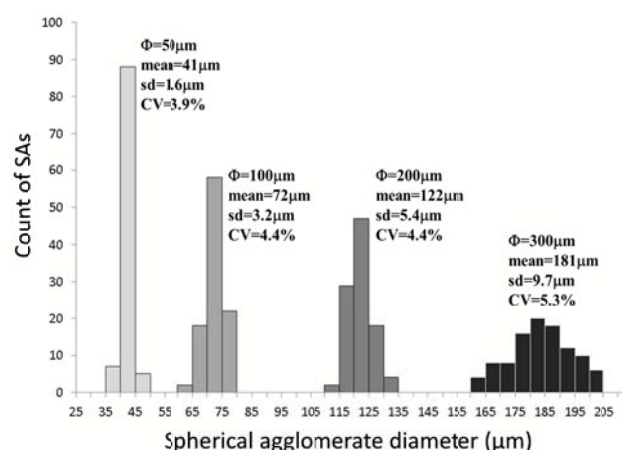
Figure 10. Size distribution of SAs in 50μm, 100μm, 200μm, and 300μm diameter microwells. The diameter of two hundred SAs was measured by analyzing crystal images. The low CV signifies that uniformity of crystal products is attained via our approach. (sd: standard deviation, CV: coefficient of variation.)

In summary, the droplet-based platform has the following distinctive advantages when compared with conventional methods, i.e. bulk solution processing, microemulsion with stirring condition, and active microfluidic-based devices: (1) better crystal quality and uniformity, i.e. narrow size distribution, (2) automatic liquid filling over the entire microwell array, (3) precise and fast temperature control due to the small droplet size, (4) static and stable dissolution process which enables control of producing various crystal forms. (A flowing droplet has internal vortices/stresses which can affect crystallization.), and (5) scalable for high throughput applications. For the above reasons we are able to produce EAs with the new droplet-based method. In conclusion, our work provides not only a flow-free droplet platform for sample package, but also an efficient temperature control over small volume solution to ensure crystal quality. This new method has great potential for pharmaceutical applications.

Conclusions

In this article, we presented a flow-free procedure to package liquid sample as droplet array, where each individual droplet is automatically placed inside a microwell without the need of other flow control mechanism. We demonstrated the advantages of this platform via the crystallization of NaCl and glycine by means of slow dissolution of water droplets. All of the products, including cubic NaCl crystals, α−, γ−, spherical and ellipsoidal crystalline agglomerates were formed in an array pattern. This scalable method has great potential to be used in pharmaceutical processes both for studying crystallization process as well as for producing large quantities of crystals.

Acknowledgements

References

1. Leon, R.A.L., et al., *Simultaneous Spherical Crystallization and Co-Formulation of Drug(s) and Excipient from Microfluidic Double Emulsions.* Crystal Growth & Design, 2013. **14**(1): p. 140-146.
2. Variankaval, N., A.S. Cote, and M.F. Doherty, *From form to function: Crystallization of active pharmaceutical ingredients.* AIChE Journal, 2008. **54**(7): p. 1682-1688.
3. Kawashima, Y., M. Okumura, and H. Takenaka, *Spherical crystallization: direct spherical agglomeration of salicylic Acid crystals during crystallization.* Science, 1982. **216**(4550): p. 1127-8.
4. Li, L. and N. Rodríguez-Hornedo, *Growth kinetics and mechanism of glycine crystals.* Journal of Crystal Growth, 1992. **121**(1–2): p. 33-38.
5. Towler, C.S., et al., *Impact of Molecular Speciation on Crystal Nucleation in Polymorphic Systems: The Conundrum of γ Glycine and Molecular 'Self Poisoning'.* Journal of the American Chemical Society, 2004. **126**(41): p. 13347-13353.
6. Rabesiaka, M., et al., *Preparation of glycine polymorphs crystallized in water and physicochemical characterizations.* Journal of Crystal Growth, 2010. **312**(11): p. 1860-1865.
7. Allen, K., et al., *The Crystallization of Glycine Polymorphs from Emulsions, Microemulsions, and Lamellar Phases.* Crystal Growth & Design, 2002. **2**(6): p. 523-527.
8. Md. Badruddoza, A.Z., et al., *Functionalized Silica Nanoparticles as Additives for Polymorphic Control in Emulsion-Based Crystallization of Glycine.* Crystal Growth & Design, 2013. **13**(6): p. 2455-2461.
9. Toldy, A.I., et al., *Spherical Crystallization of Glycine from Monodisperse Microfluidic Emulsions.* Crystal Growth & Design, 2012. **12**(8): p. 3977-3982.
10. Chadwick, K., et al., *Crystallisation from Water-in-Oil Emulsions As a Route to Spherical Particulates: Glycine and the Hydrochloride Salts of Glutamic Acid and Ephedrine.* Organic Process Research & Development, 2009. **13**(6): p. 1284-1290.
11. Pompano, R.R., et al., *Microfluidics Using Spatially Defined Arrays of Droplets in One, Two, and Three Dimensions.* Annual Review of Analytical Chemistry, 2011. **4**(1): p. 59-81.
12. Clausell-Tormos, J., et al., *Droplet-Based Microfluidic Platforms for the Encapsulation and Screening of Mammalian Cells and Multicellular Organisms.* Chemistry & biology, 2008. **15**(5): p. 427-437.
13. Shi, W., et al., *Droplet-based microfluidic system for individual Caenorhabditis elegans assay.* Lab on a Chip, 2008. **8**(9): p. 1432-1435.
14. Du, W., et al., *SlipChip.* Lab on a Chip, 2009. 9(16): p. 2286-2292.
15. Um, E., et al., *Mesh-integrated microdroplet array for simultaneous merging and storage of single-cell droplets.* Lab on a Chip, 2012. **12**(9): p. 1594-1597.
16. Lee A Y, Lee I S, Dette S S, et al. *Crystallization on confined engineered surfaces: A method to control crystal size and generate different polymorphs.* Journal of the American Chemical Society, 2005, 127(43): 14982-14983.
17. Zhu, Q., et al., *Self-priming compartmentalization digital LAMP for point-of-care.* Lab on a Chip, 2012. **12**(22): p. 4755-4763.
18. Dimov, I.K., et al., *Stand-alone self-powered integrated microfluidic blood analysis system (SIMBAS).* Lab on a Chip, 2011. **11**(5): p. 845-850.
19. Shim, J.-u., et al., *Using Microfluidics to Decouple Nucleation and Growth of Protein Crystals†.* Crystal Growth & Design, 2007. **7**(11): p. 2192-2194.
20. Casadevall i Solvas, X., et al., *Microfluidic evaporator for on-chip sample concentration.* Lab on a Chip, 2012. **12**(20): p. 4049-4054.
21. Weissbuch, I., L. Leisorowitz, and M. Lahav, *"Tailor-Made" and charge-transfer auxiliaries for the control of the crystal polymorphism of glycine.* Advanced Materials, 1994. **6**(12): p. 952-956.
22. Dowling, R., et al., *Acceleration of crystal growth rates: an unexpected effect of tailor-made additives.* Chemical Communications, 2010. **46**(32): p. 5924-5926.
23. Chew, J.W., et al., *Stable polymorphs: difficult to make and difficult to predict.* CrystEngComm, 2007. **9**(2): p. 128-130.
24. Bouchard, A., et al., *Ways of manipulating the polymorphism of glycine during supercritical fluid crystallisation.* The Journal of Supercritical Fluids, 2008. **44**(3): p. 422-432.